Inorg. Chem. **2003**, *42*, 8579–8584

Dinuclear and Octanuclear Mn(II) Complexes with μ^2-C, μ^2-N(Pyrrolide), and μ-η^1:η^5-(Pyrrolide) Bridges: A Structural and Magnetic Study

Patrick Crewdson,[†] Sandro Gambarotta,*[,†] Glenn P. A. Yap,[†] and Laurence K. Thompson*[,‡]

Departments of Chemistry, University of Ottawa, Ottawa, Ontario K1N 6N5, Canada, and Memorial University, St John's, Newfoundland A1B 3X7, Canada

Received August 1, 2003

Reaction of the dinuclear $[(CH_2SiMe_3)(\mu\text{-}CH_2SiMe_3)Mn(THF)]_2$ (**1**) with an equivalent amount of 1,1-dipyrrolylcyclohexane afforded two compounds depending on the solvent employed. Reaction carried out in THF afforded the dinuclear $\{[1,1\text{-}(\mu\text{-}C_4H_3N)(C_4H_3N)C_6H_{10}]Mn(THF)_2\}_2\cdot 2(THF)$ (**2**) while reaction in toluene yielded the octanuclear and cyclic cluster $\{[1,1\text{-}(\mu,\eta^1\text{:}\eta^5\text{-}C_4H_3N)_2C_6H_{10}]Mn\}_8\cdot 4(toluene)$ (**3**). The magnetism in all three cases is dominated by intramolecular antiferromagnetic exchange with strong coupling in **1** ($J = -85$ cm^{-1}), and in **2** ($J = -23.2$ cm^{-1}), whereas substantially weaker coupling through the σ/π-bonded dipyrrolide bridges ($J = -3.3$ cm^{-1}) was observed within the cyclic and octameric **3**.

Introduction

There are many reasons for interest in the chemistry of multinuclear divalent manganese complexes of N-donor based ligand systems. For example, these species display a great ability to work as both oxygen transfer and epoxidation catalysts,[1] but among the most appealing features certainly there is the ability of a tetranuclear manganese cluster to perform the water oxidation process in green plants.[2] With the ultimate goal of building new model compounds for photochemical O−H bond oxidation or CO_2 activation, we became interested in the preparation, characterization, and redox chemistry of manganese clusters supported by dipyrrolide ligands.

In particular, the aim of this preliminary study was to test the hypothesis that dipyrrolide dianions might be promising ligands for the purpose of preparing reactive, yet hydrolysis resistant, clusters. In turn, these species might give accessibility to a family of higher valent clusters with the possibility of cooperative interactions of several metal centers with the same target molecule. Among the salient characteristics that make dipyrrolide dianions versatile and promising ligands is the possibility for the two rings to adopt both σ- and π-bonding modes, thus providing the metal with a remarkable steric and electronic flexibility. In lanthanide chemistry[3] these systems have been shown to be capable of (1) supporting a very high level of chemical reactivity;[4] (2) assembling both polymeric and cluster structures of different nuclearity depending on the nature of the ligand substituents;[5] (3) retaining alkali cations that, by coordinating to the rings' either σ- or p-orbitals, modify the electron-donating ability of the ligand,[6] ultimately affecting the metal redox potential; and (4) substantially increasing the reactivity of the metal center.[7]

* Author to whom correspondence should be addressed. E-mail: sgambaro@science.uottawa.ca. Tel: (613) 562-5199. Fax: (613) 562-5170.
[†] University of Ottawa.
[‡] Memorial University.

(1) (a) Daly, A. M.; Gilheany, D. G. *Tetrahedron: Asymmetry* **2003**, *14*, 127. (b) Mansuy, D. *Coord. Chem. Rev.* **1993**, *125*, 129. (c) Gazeau, S.; Pecaut, J.; Haddad, R.; Shelnutt, J. A.; Marchon, J. *Eur. J. Inorg. Chem.* **2002**, *11*, 2956. (d) Havranek, M.; Singh, A.; Sames, D. *J. Am. Chem. Soc.* **1999**, *121*, 8965.
(2) (a) Nugent, J. H. A.; Rich, A. M.; Evans, M. C. W. *Biochim. Biophys. Acta* **2001**, *138*, 1503. (b) Dau, H.; Iuzzolino, L.; Dittmer, J. *Biochim. Biophys. Acta* **2001**, *24*, 1503. (c) Cinco, R. M.; Rompel, A.; Visser, H.; Aromý, G.; Christou, G.; Sauer, K.; Klein, M. P.; Yachandra, V. K. *Inorg. Chem.* **1999**, *38*, 5988. (d) Philouze, C.; Blondin, G.; Girerd, J.; Guilhem, J.; Pascard, C.; Lexa, D. *J. Am. Chem. Soc.* **1994**, *116*, 8557.
(3) Dubé, T.; Conoci, S.; Gambarotta, S.; Yap, G. P. A.; Vasapollo, G. *Angew. Chem., Int. Ed.* **1999**, *38*, 3657.
(4) (a) Aharonian, G.; Gambarotta, S.; Yap, G. P. A. *Organometallics* **2002**, *21*, 4257. (b) Dubé, T.; Ganesan, M.; Conoci, S.; Gambarotta, S.; Yap, G. P. A *Organometallics* **2000**, *19*, 3716.
(5) (a) Freckmann, D. M. M.; Dubé, T.; Berube, C. D.; Gambarotta, S.; Yap, G. P. A. *Organometallics* **2002**, *21*, 1240. (b) Dubé, T.; Freckmann, D.; Conoci, S.; Gambarotta, S.; Yap, G. P. A. *Organometallics* **2000**, *19*, 209. (c) Dubé, T.; Gambarotta, S.; Conoci, S.; Yap, G. P. A *Organometallics* **2000**, *19*, 115. (d) Dubé, T.; Gambarotta, S.; Conoci, S.; Yap, G. P. A *Organometallics* **2000**, *19*, 1182.
(6) (a) Mani, G.; Berube, C. D.; Gambarotta, S.; Yap, G. P. A. *Organometallics* **2002**, *21*, 1707. (b) Dubé, T.; Gambarotta, S.; Yap, G. P. A. *Angew. Chem., Int. Ed.* **1999**, *38*, 1432.
(7) Mani, G.; Gambarotta, S.; Yap, G. P. A. *Angew. Chem., Int. Ed.* **2001**, *40*, 766.

10.1021/ic0349205 CCC: $25.00
Published on Web 11/15/2003

In this paper we wish to describe the preparation of a new Mn(II) dialkyl complex and of two novel dipyrrolide derivatives, which are a rare example of high-nuclearity Mn(II) compounds,[8] together with an assessment of their magnetic properties.

Experimental Section

All reactions were carried out under a dry nitrogen atmosphere. Solvents were dried using an aluminum oxide solvent purification system. 1,1-Dipyrrolylcyclohexane[9] and $LiCH_2Si(CH_3)_3$[10] were prepared according to published procedures. Infrared spectra were recorded on a Mattson 9000 and Nicolet 750-Magna FTIR instruments from Nujol mulls prepared in a drybox. Samples of **1** and **2** for magnetic susceptibility measurements were preweighed inside a drybox equipped with an analytical balance and flame sealed into calibrated 5 mm "o.d." quartz tubes. Magnetic measurements were carried out using a Quantum Design MPMS5S SQUID magnetometer at 0.1 T, in the temperature range 2−300 K. The accurate sample mass was determined by difference by breaking the tube after data collection. Background data on the cleaned, empty tube were obtained under identical experimental conditions. **3** was weighed into a standard "gelcap" and sealed in a glass tube in the drybox for shipment. The "gelcap" was sealed with "Kapton" tape on breaking the glass tube, and quickly loaded into the SQUID magnetometer. Background corrections for the "gelcap" were included in the magnetic calculations. Standard corrections for underlying diamagnetism were applied to data.[11] Elemental analyses were carried out with a Perkin-Elmer 2400 CHN analyzer. Data for X-ray crystal structure determination were obtained with a Bruker diffractometer equipped with a Smart CCD area detector.

Synthesis of $[Mn(CH_2Si(Me_3)(\mu\text{-}CH_2SiMe_3)(THF)]_2$ (1). $[MnCl_2(THF)_2]$ (5.5 g, 20.4 mmol) was suspended in 30 mL of Et_2O and cooled at −35 °C for 30 min. $LiCH_2SiMe_3$ (4.0 g, 42.9 mmol) was dissolved in 50 mL Et_2O and cooled at −35 °C for 30 min. The two solutions were combined yielding a cloudy pink mixture, which was stirred for 12 h at room temperature. The solvent was then removed in vacuo, and 50 mL of hexanes was added, resulting in a dark orange solution with a white precipitate. The suspension was filtered and the resulting solution allowed to stand at −35 °C for 12 h. Orange crystals of **1** suitable for X-ray diffraction separated (5.5 g, 9.1 mmol, 89%). IR (Nujol) ν: 1294 (w), 1245 (s), 998 (m), 917 (s), 897 (s) 843 (s), 743 (s), 700 (s), 680 (s), 607 (m), 446 (s). Elemental analysis calculated (%) for $Mn_2C_{24}H_{60}Si_4O_2$: C 47.81, H 10.03. Found: C 47.73, H 9.92.

Synthesis of $\{[(\mu\text{-}C_4H_3N)(C_4H_3N)C_6H_{10}]Mn(THF)_2\}_2\cdot 2(THF)$ (2). The addition of THF (15 mL) to a mixture of solid 1,1-dipyrrolylcyclohexane (0.09 g, 0.40 mmol) and **1** (0.12 g, 0.20 mmol) in a vial resulted in the formation of a clear colorless solution. Light pink crystals of **2** suitable for X-ray diffraction were formed upon standing for 24 h at room temperature (0.15 g, 0.15 mmol, 75%). IR (Nujol) ν: 3088 (w), 3086 (w), 1164 (w), 1127 (w), 1065 (m), 1030 (s), 965 (w), 952 (w), 905 (m), 874 (m), 829 (w), 738 (m), 726 (m), 714 (m), 631 (w). Elemental analysis calculated (%) for $Mn_2C_{52}H_{80}N_4O_6$: C 64.58, H 8.34, N 5.79. Found: C 64.55, H 8.29, N 5.69.

Synthesis of $\{[1,1\text{-}(\mu\text{-}\eta^4\text{:}\eta^1C_4H_3N)_2C_6H_{10}]Mn\}_8\cdot 4(toluene)$ (3). A mixture of solid 1,1-dipyrrolylcyclohexane (0.07 g, 0.34 mmol) and **1** (0.10 g, 0.16 mmol) was placed in a vial, and 10 mL of toluene was added, resulting in a colorless solution. Clear crystals of **3** suitable for X-ray diffraction separated upon allowing the solution to stand for 24 h at room temperature (0.096 g, 0.04 mmol, 96%). IR (Nujol) ν: 3370 (w), 3088 (w), 1609 (w), 1300 (w), 1272 (m), 1200 (s), 1161 (s), 1129 (s), 1106 (m), 1033 (s), 965 (m), 906 (m), 872 (w), 851 (w), 830 (w), 790 (s), 744 (s), 693 (m), 621 (m). Elemental analysis calculated (%) for $Mn_8C_{140}H_{160}N_{16}$: C 67.09, H 6.43, N 8.94. Found C 67.01, H 6.39, N 8.88.

X-ray Crystallography. Suitable crystals were selected, mounted on a thin, glass fiber using paraffin oil, and cooled to the data collection temperature. Data were collected on a Bruker AXS SMART 1k CCD diffractometer using 0.3° ω-scans at 0°, 90°, and 180° in ϕ. Initial unit-cell parameters were determined from 60 data frames collected at different sections of the Ewald sphere. Semiempirical absorption corrections based on equivalent reflections were applied.[12]

The systematic absences and unit-cell parameters were uniquely consistent for the reported space groups. The structures were solved by direct methods, completed with difference Fourier syntheses, and refined with full-matrix least-squares procedures based on F^2. The compound molecule is located on an inversion center for **1** and **2**, and on a 2-fold rotation axis for **3**. A molecule of cocrystallized tetrahydrofuran (THF) solvent was located in the asymmetric unit of **2**. Two molecules of cocrystallized toluene solvent were located rotationally disordered in the asymmetric unit of **3** with refined site occupancy distributions of 50/50 and 90/10. The coordinated THF molecule in **1** was disordered such that one carbon atom was located in two positions with a refined site occupancy distribution of 60/40. All the non-hydrogen atoms were refined with anisotropic displacement parameters excepting the methyl carbon atom of the first disordered toluene molecule and the atoms of the second disordered toluene molecule in **3** and which were refined isotropically. The methyl carbon atoms of the disordered toluene molecules in **3** were assigned equal isotropic atomic displacement parameters for each contributing disordered pair. The phenyl groups of the toluene molecules in **3** were refined as rigid hexagons. All hydrogen atoms were treated as idealized contributions. All scattering factors are contained in the SHELXTL 6.12 program library. Relevant crystallographic data and bond distances and angles are reported in Tables 1 and 2, respectively.

Results and Discussion

For the purpose of avoiding the presence of alkali cations that might lead to monomeric *-ate* types of structures, it was decided to react homoleptic Mn(II) alkyls with 1,1-dipyrrolylcyclohexane. For this purpose, the homoleptic and polymeric $[Mn(CH_2SiMe_3)(\mu\text{-}CH_2SiMe_3)]_n$ claimed in the literature[13] seemed to be a particularly versatile starting material given the volatility of the TMS group expected to

(8) (a) Alvarez, C. S.; Bond, A. D.; Cave, D.; Mosquera, M. E. G.; Harron, E. A.; Layfield, R. A.; McPartlin, M.; Rawson, J. M.; Wood, P. T.; Wright, D. S. *J. Chem. Soc., Chem. Commun.* **2002**, 2980. (b) Soria Alvarez, A.; Bond, A. D.; Harron, E. A.; Layfield, R. A.; McAllister, J. A.; Pask, C. M.; Rawson, J. M.; Wright, D. S. *Organometallics* **2001**, *20*, 4135.

(9) (a) Dolphin, D.; Liu, B. Y.; Bruckner, C. *Chem. Commun*. **1996**, 2141. (b) Lee, C. H.; Lindsey, S. *Tetrahedron* **1994**, *50*, 11427. (c) Brown, W. H.; Hutchinson, B. J.; MacKinnon, M. H. *Can. J. Chem.* **1971**, *49*, 4017.

(10) Peterson, D. J. *J. Organomet.* **1967**, *9*, 373.

(11) (a) Mabbs, M. B.; Machin, D. *Magnetism and Transition Metal Complexes*; Chapman and Hall: London, 1973. (b) Foese, G.; Gorter, C. J.; Smits, L. J. *Constantes Selectionnes, Diamagnetisme, Paramagnetism, Relaxation Paramagnetique*; Masson: Paris, 1957.

(12) Blessing, R. *Acta Crystallogr.* **1995**, *A51*, 33.

(13) Anderson, R. A.; Carmona-Guzman, E.; Gibson, J. F.; Wilkinson, G. J. *J. Chem. Soc., Dalton Trans.* **1976**, 2204.

Table 1. Crystal Data and Structure Analysis Results

	1	2	3
formula	$Mn_2C_{24}H_{60}O_2Si_4$	$Mn_2C_{52}H_{80}N_4O_5$	$Mn_8C_{140}H_{160}N_6$
fw	602.96	951.11	2506.36
crystal system	monoclinic	monoclinic	orthorhombic
space group	*P*2(1)/*c*	*P*2(1)/*c*	*Pbcn*
a (Å)	10.1991(16)	10.6733(11)	26.483(9)
b (Å)	15.568(2)	11.8769(13)	20.351(7)
c (Å)	12.747(2)	19.867(2)	23.459(8)
α (deg)	90	90	90
β (deg)	113.482(2)	97.054(2)	90
γ (deg)	90	90	90
V (Å^3)	1856.4(5)	2499.4(5)	12643(7)
Z	2	2	4
radiation (Kα, Å)	0.71073	0.71073	0.71073
T (K)	203(2)	203(2)	203(2)
D_{calcd} (g cm^{-3})	1.079	1.285	1.317
μ_{calcd} (mm^{-1})	0.825	0.557	0.828
F_{000}	652	1036	5248
R, wR2	0.0488, 0.1300	0.0503, 0.1379	0.0603, 0.1339
GOF	1.048	1.023	1.038

[a] $R = \sum||F_o| - |F_c||/\sum|F_o|$. $wR2 = [\sum(|F_o| - |F_c|)^2/(\sum wF_o^2)]^{1/2}$.

form upon protonolysis by the dipyrrole ligand. However, due to its incomplete characterization in the original literature preparation, an alternate synthesis was used. By using the lithium derivative $LiCH_2SiMe_3$ instead of the corresponding Grignard for the direct reaction with $MnCl_2(THF)_2$, the new dinuclear complex $[Mn(CH_2SiMe_3)(\mu\text{-}CH_2SiMe_3)(THF)]_2$ (**1**) was obtained. The complex was readily prepared by treating $MnCl_2(THF)_2$ with two equivalents of $LiCH_2Si(CH_3)_3$ in Et_2O and was isolated in high yield as exceedingly air-sensitive dark-orange crystals upon extraction with hexanes of the evaporated reaction mixture, followed by crystallization at low temperature.

The crystal structure of **1** (Figure 1) consists of a symmetry-generated dimer where two tetrahedral divalent Mn centers are connected in an overall edge-sharing bitetrahedral structure. The bridging interaction between the two metal centers is provided by the CH_2 groups of two bridging alkyls [Mn−C−Mn(a) = 75.07(9)°, Mn(a)−C = 2.360(3) Å, Mn−C 2.214(3) Å]. The bridging carbon atom displays a curious T-shape coordination with the Si and the two Mn atoms [Si(2)−C(5)−Mn(a) = 175.92(13)°, Si(2)−C(5)−Mn = 106.03(13)°, Mn−C(5)−Mn(a) = 75.07(9)°] as derived from a trigonal bipyramid where the idealized positions of

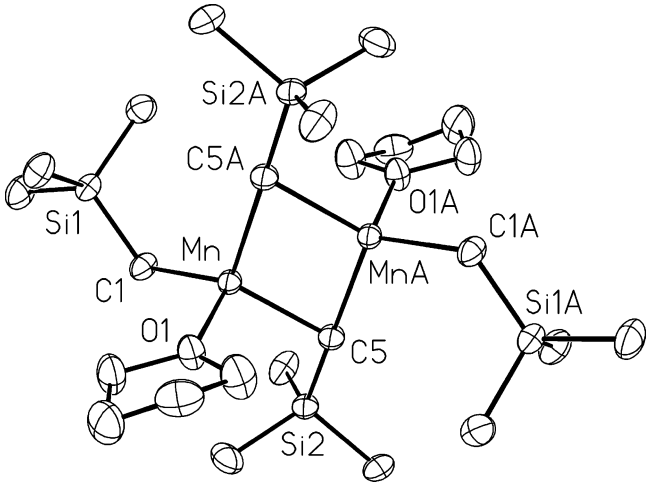

Figure 1. Thermal ellipsoid plot of **1**. Thermal ellipsoids are drawn at 30% probability.

two hydrogen atoms and the second Mn atom define the equatorial plane, and the second Mn and the Si atom being on the two axial positions. The tetrahedral structure around each Mn center is completed by one terminally bound alkyl group [Mn−C(1) = 2.129(3) Å] and one molecule of THF [C(1)−Mn−O(1)=108.19(11)°, C(1)−Mn−C(5)=127.30(11)°, C(1)−Mn−C(5a)=115.94(11)°, O(1)−Mn−C(5)=99.19(10)°, O(1)−Mn−C(5a)=94.73(10)°, C(5)−Mn−C(5a)=105.28(10)°].

The Mn−Mn distance [Mn−Mn(a) = 2.7878(9) Å] is rather short and might be regarded as falling into what is normally regarded as the M−M bonding range. The complex is paramagnetic showing the typical dependence of magnetic susceptibility as a function of temperature (Figure 2) expected for an antiferromagnetically coupled dinuclear complex. The magnetic susceptibility has a broad, flat maximum at ∼150 K, with a sharp rise at low temperature indicative of the presence of a small amount of paramagnetic impurity. The data were satisfactorily fitted to an exchange expression for a simple dinuclear Mn(II) system ($H = -J\{S_1 \cdot S_2\}$; $S = {}^5/_2$) using MAGMUN-4.0,[14] giving $g = 2.01(5)$, $J = -85$ (4) cm^{-1}, TIP = 44 × 10^{-6} cm^3·mol^{-1}, $\rho = 0.011$, $\theta = 0$ K ($10^2R = 1.98$; $R = [\sum(\chi_{obs} - \chi_{calc})^2/\sum\chi_{obs}^2]^{1/2}$; ρ = fraction paramagnetic impurity, θ = Weiss-like temperature correction, TIP = temperature independent paramagnetism). The

Table 2. Selected Bond Distances (Å) and Angles (deg)

1		2		3	
Mn−Mn(a)	2.7878(9)	Mn−Mn(a)	3.2033(7)	Mn(1)−Mn(2)	4.074
Mn−C(1)	2.129(3)	Mn−N(1)	2.089(2)	Mn(2)−Mn(3)	4.015
Mn−C(5)	2.214(3)	Mn−N(2a)	2.1954(18)	Mn(3)−Mn(4)	4.033
Mn(1)−C(5)	2.360(3)	Mn−N(2)	2.3211(19)	Mn(4)−Mn(1a)	4.113
Mn−C(5)−Mn(a)	75.07(9)	Mn−N(2)−Mn(a)	90.31(7)	Mn(1)−N(4)	2.116(5)
Si(2)−C(5)−Mn	175.92(13)	O(1)−Mn−O(2)	79.92(6)	Mn(1)−N(1)	2.117(5)
Si(2)−C(5)−Mn(a)	106.03(13)	O(1)−Mn−N(1)	98.52(7)	Mn(2)−N(6)	2.134(5)
C(1)−Mn−O(1)	108.19(11)	O(1)−Mn−N(2)	165.43(7)	Mn(2)−N(3)	2.134(5)
C(1)−Mn−C(5)	127.30(11)	O(1)−Mn−N(2a)	92.71(7)	Mn(3)−N(5)	2.119(5)
C(1)−Mn−C(5a)	115.94(11)	O(2)−Mn−N(1)	99.27(7)	Mn(3)−N(8)	2.123(5)
C(5)−Mn−C(5a)	105.28(10)	O(2)−Mn−N(2)	90.24(7)	Mn(4)−N(7)	2.118(5)
O(1)−Mn−C(5)	99.19(10)	O(2)−Mn−N(2a)	146.83(7)	Mn(4)−N(2a)	2.135(5)
O(1)−Mn−C(5a)	94.73(10)	N(1)−Mn−N(2)	93.62(7)	N(1)−Mn(1)−N(4)	113.34(19)
		N(1)−Mn−N(2a)	113.84(8)	N(3)−Mn(2)−N(6)	115.22(19)
		N(2)−Mn−N(2a)	89.69(7)	N(5)−Mn(3)−N(8)	117.5(2)
				N(7)−Mn(4)−N(2a)	120.1(2)

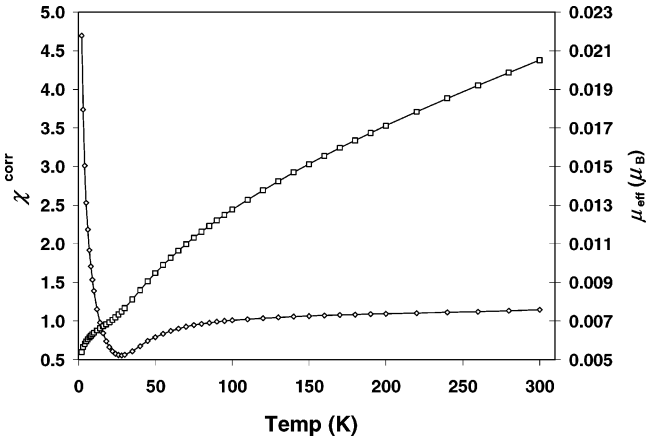

Figure 2. Diagram of the magnetic susceptibility (◇) and of the magnetic moment (□) versus T for **1**.

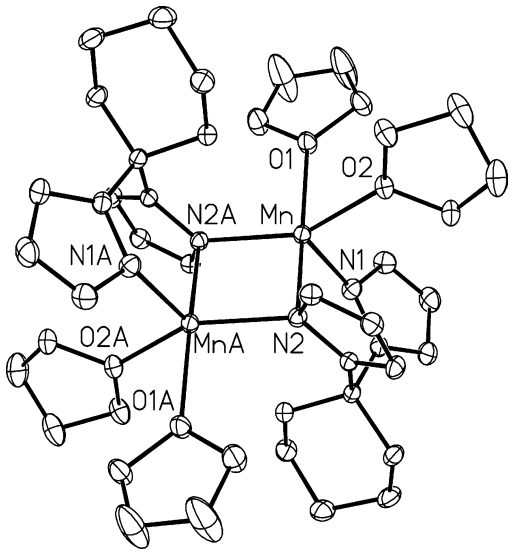

Figure 3. Thermal ellipsoid plot of **2**. Thermal ellipsoids are drawn at 30% probability.

solid lines in Figure 2 were calculated with these parameters. Such strong antiferromagnetic coupling between the two Mn centers is unprecedented to the best of our knowledge. A d^5-d^5 dinuclear system has low probability of forming a M−M bond that at most will be a single bond with a $\sigma^2\pi^2\delta^2\delta^{*2}\pi^{*2}$ ground state.[15] The presence of substantial paramagnetism even at zero K suggests that in this case the Mn−Mn interaction is exclusively limited to antiferromagnetic exchange and not even a M−M single bond exists despite the substantially short Mn−Mn distance.

The reaction of **1** with 1,1-dipyrrolylcyclohexane ligand afforded two completely different compounds depending on the nature of the solvent employed. The reaction carried out in THF afforded the dinuclear $\{[1,1\text{-}(\mu\text{-}C_4H_3N)(C_4H_3N)\text{-}C_6H_{10}]Mn(THF)_2\}_2\cdot 2(THF)$ (**2**) that was isolated in high yield as very air-sensitive, pale-pink crystals upon allowing the reaction mixture to stand at room temperature overnight.

The symmetry-generated dinuclear arrangement was revealed by an X-ray crystal structure (Figure 3) and consists of two identical Mn(ligand)$(THF)_2$ units in which each Mn(II) atom adopts a distorted square pyramidal coordination geometry [O(1)−Mn−O(2) = 79.92(6)°, O(1)−Mn−N(1) = 98.52(7)°, O(1)−Mn−N(2) = 165.43(7)°, O(1)−Mn−N(2a) = 92.71(7)°, O(2)−Mn−N(1) = 99.27(7)°, O(2)−Mn−N(2) = 90.24(7)°, O(2)−Mn−N(2a) = 146.83(7)°, N(1)−Mn−N(2) = 93.62(7)°, N(1)−Mn−N(2a) = 113.84(8)°, N(2)−Mn−N(2a) = 89.69(7)°]. The bridging between the two metal centers is provided by two μ^2-N pyrrolide rings, each from one of the two ligands, and exclusively using the ring N atom [Mn−N(2)−Mn(a) = 90.31(7)°] as a bridge linking the equatorial positions of the two metal centers [Mn−N(2) = 2.3211(19) Å, Mn−N(2a) = 2.1954(18) Å]. The second pyrrolyl ring of each ligand is σ-bonded to an axial position of each Mn atom [Mn−N(1) = 2.089(2) Å]. The remaining equatorial positions of each Mn atom are occupied by two molecules of THF. The Mn···Mn nonbonding distance [Mn···Mn(a) = 3.2033(7) Å] is quite long and rules out the presence of a direct Mn−Mn bonding interaction.

The same reaction carried out in toluene, rather than in THF, afforded a colorless solution from which colorless crystals of the octanuclear complex $\{[1,1\text{-}(\mu\text{-}\eta^1\text{:}\eta^4\text{-}C_4H_3N)_2\text{-}C_6H_{10}]Mn\}_8\cdot 4(toluene)$ (**3**) were obtained upon allowing the reaction mixture to stand for a few hours at room temperature. Complex **3** could also be obtained from **2** by dissolving it into boiling toluene with a subsequent crystallization, whereas boiling **3** in THF formed **2**. Therefore, the two complexes can reversibly be transformed into each other depending on the nature of the solvent. This possibly suggests the existence of equilibria between solution and solid state and association/dissociation equilibria of Lewis bases. We found no evidence for the existence of different nuclearity cluster (hexamers, pentamers, etc.). Attempts to use different solvents to prove the effect of the Lewis basicity on cluster nuclearity did not provide good crystals to substantiate the point.

The structure of **3** consists of an octanuclear, cyclic structure (Figure 4a) with the eight Mn atoms (each formally having a 21-electron configuration) being nearly coplanar and forming a regular ring (Figure 4b). The dipyrrolide ligand adopts the same bridging bonding mode observed in similar

(14) MAGMUN4.0 is available free of charge from http://www.ucs.mun.ca/~lthomp/index.html. It has been developed by Dr. Zhiqiang Xu (Memorial University), in conjunction with Dr. O. Waldmann (waldmann@mps.ohio-state.edu). We do not distribute the source codes. Total spin state values (S'), and their energies, based on the appropriate exchange Hamiltonian, are computed within the software using normal procedures, and are substituted into the van Vleck equation (eq 1), which is corrected for TIP, θ (Weiss-like correction), and ρ (paramagnetic impurity fraction) (eq 1, 2). The programs may be used only for scientific purposes, and economic utilization is not allowed. If the routine is used to obtain scientific results, which are published, the origin of the programs should be quoted.

$$\chi_{M'} = \frac{N\beta^2 g^2}{3k(T-\theta)} \frac{\sum S'(S'+1)(2S'+1)e^{-E(S')/kT}}{\sum (2S'+1)e^{-E(S')/kT}} \quad (1)$$

$$\chi_M = \chi_{M'}(1-\rho) + \frac{4S(S+1)N\beta^2 g^2 \rho}{3kT} + \text{TIP} \quad (2)$$

(15) (a) Cotton, F. A.; Walton, R. A. *Multiple bonds between metal atoms*, 2nd ed.; Clarendon Press: Oxford, 1993. (b) Cotton, F. A.; Wilkinson, G.; Murillo, C. A.; Bochmann, M. *Advanced Inorganic Chemistry*, 6th ed.; Wiley: New York, 1999.

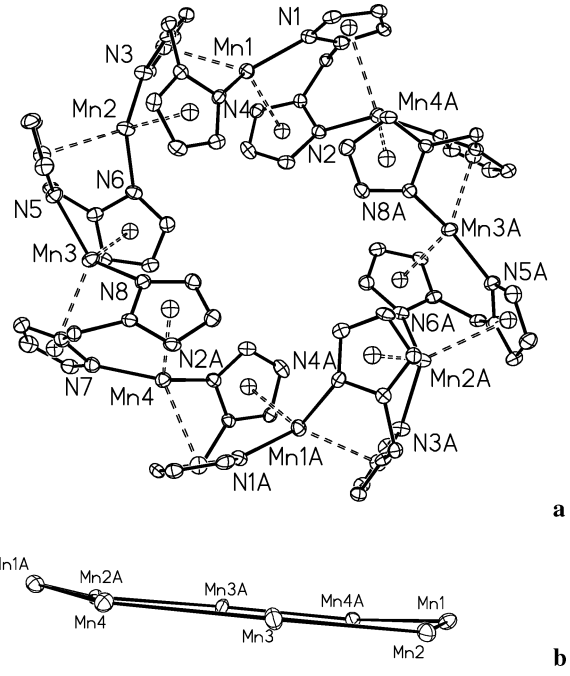

Figure 4. Thermal ellipsoid plot of **3**. Thermal ellipsoids are drawn at 30% probability, and side groups are removed for clarity (a). Plot showing the arrangement of the metal atoms only (b).

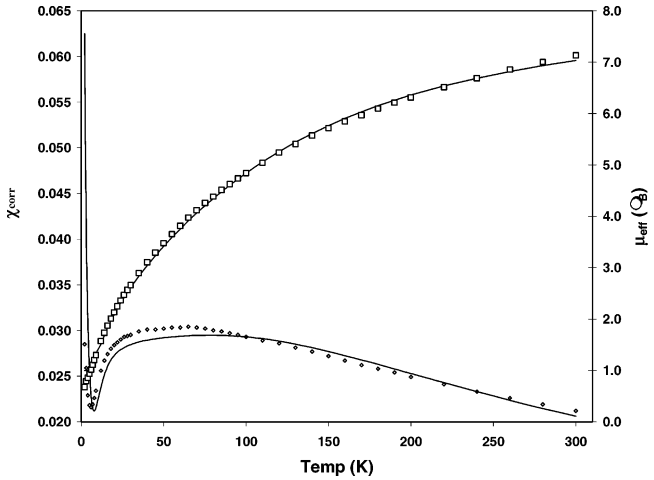

Figure 5. Diagram of the magnetic susceptibility (◇) and of the magnetic moment (□) versus T for **2**.

cluster structures of lanthanides[7] with the pyrrolide rings being σ-bonded to one metal atom and π-bonded to the next. Each Mn(II) ion adopts a pseudotetrahedral coordination geometry defined by the centroids of two π-bonded rings from two different ligands and σ-bonded N atoms of two other rings also from the two ligands. The Mn−Mn distances between two contiguous Mn atoms fall between 4.015 and4.113 Å. A large circular void exists inside the ring with a diameter of ∼10 Å. It should also be noted that the cluster is remarkably thermally robust in boiling toluene, though it still exhibits air sensitivity.

The magnetic properties of the two complexes show that both exhibit intramolecular antiferromagnetic exchange. Complex **2** shows a plot of molar susceptibility as a function of temperature (Figure 5) with a broad maximum at about 50 K, with a sharp rise at low temperature indicative of the

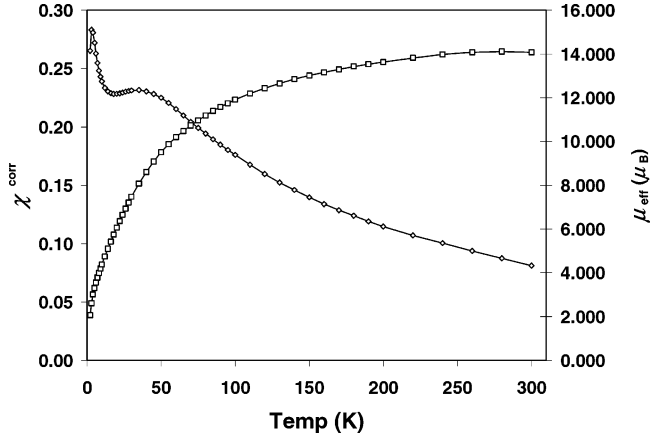

Figure 6. Diagram of the magnetic susceptibility (◇) and of the magnetic moment (□) versus T for **3**.

presence of a small amount of paramagnetic impurity. The data were fitted to a simple isotropic exchange expression for a dinuclear Mn(II) system ($H = -J\{S_1 \cdot S_2\}$) using MAGMUN-4.0[14] to give $g = 2.02(1)$, $J = -23.2(4)$ cm^{-1}, TIP $= 20 \times 10^{-6}$ cm^3·mol^{-1}, $\rho = 0.014$, $\theta = 0$ K ($10^2R = 1.87$)]. The solid line in Figure 5 was calculated with these parameters. Fitting was found to be difficult near the maximum in χ_M, but overall the fitting parameter is reasonable. This can be associated with the difficulty of getting highly accurate background correction data for the quartz tube. Conditions were optimized in this context by running the sample and background data collections very slowly to ensure good thermal equilibration, and by placing the empty tube in the sampling position as close as possible to the original. Figure 5 shows the fitted plot of magnetic moment (per mole) as a function of temperature.

The behavior of the magnetic susceptibility of the octanuclear complex **3** as a function of the temperature shows the characteristic maximum at 35 K also indicative of the presence of intramolecular antiferromagnetic exchange (Figure 6). The rise in χ_M at low temperature again signals a small proportion of paramagnetic impurity, typical in large clusters. The magnetic moment per mole displays normal behavior for such a system rising from 3.13 μ_B at 4 K to a maximum value of 14.7 μ_B at 300 K (Figure 6). This is indicative of an antiferromagnetic/superexchange process through the pyrrolide fragments. The room temperature moment is somewhat lower than that expected for eight uncoupled Mn(II) centers ($g = 2$, 16.7 μ_B). The magnetic data (per mole) were not fitted to an exchange model based on a ring of eight Mn(II) ($S = {}^5/_2$) centers, because of the computing difficulties of dealing with such a large calculation. Instead, since the ring is large, and approximates a 1-dimensional chain, the data were fitted to a 1-dimensional chain model[16] assuming a classical spin vector assembly of $S = {}^5/_2$ centers. A successful fit was obtained with $g = 1.96(2)$, $J = -3.4(2)$ cm^{-1}, $\rho = 0.015$, TIP $= 0$ cm^3·mol^{-1}, $\theta = 0$ K ($10^2R = 3.0$)]. The solid lines in Figure 6 were calculated with these parameters. The Mn(II) centers are therefore coupled uniformly throughout the ring with a

(16) Fisher, M. E. *Am. J. Phys.* **1964**, *32*, 343.

moderate exchange integral, and coupling may occur (given the long Mn···Mn nonbonding distance) through the two types of pyrrolide bridging ligands connecting each adjacent pair of metal ions (superexchange). Definite information about the strength of the ligand field induced by a π-bonded pyrrolide ring is not available, and thus the possibility that an intermediate spin state might provide a more correct description for Mn(II) in the type of coordination environment existing in **3** cannot confidently be excluded. Nevertheless, it seems questionable in light of the tetrahedral coordination environment.

Summary

In summary, we have synthesized three antiferromagnetically coupled divalent Mn compounds. The organometallic **1** displays a very strong antiferromagnetic coupling which rules out the presence of a Mn−Mn single bond. The sharing of a bridging nitrogen atom in **2** and the consequent short Mn−Mn distance also result in a strong antiferromagnetic coupling although substantially smaller than in the case of **1**. Although this might be taken as an indication for the presence of a superexchange mechanism, it is difficult to attribute this difference simply to the different nature of the two donor atoms (C versus N) given that in the two complexes the Mn−Mn distance varies rather substantially as a result of geometry optimization as required by the two different ligand systems (alkyl versus dipyrrolide). The different bonding modes of the dipyrrolide ligand, μ-N versus $\mu,\eta^1{:}\eta^5$ pyrrolyl as displayed by **2** and **3**, is certainly responsible for the dramatic structural change and variationof the Mn···Mn distance, which ultimately changes the magnitude of magnetic coupling. The ability of the ligand to determine this spectacular variation depending on bonding mode is remarkable and opens interesting perspectives. The critical point is of course how to control the bonding mode of the ligand to the metal that causes such a substantial variation of magnetism. In the particular case presented above this is simply achieved by the reversible coordination/elimination of a weak Lewis base (THF).

Acknowledgment. This work was supported by the Natural Sciences and Engineering Council of Canada (NSERC) and by the Canada Foundation for Innovation (CFI) through an infrastructure grant.

Supporting Information Available: Magnetism data and listings of atomic coordinates, thermal parameters, and bond distances and angles for the structures reported in this work. This material is available free of charge via the Internet at http://pubs.acs.org.

IC0349205